

LIDAR-ACOUSTIC STUDIES OF METEOROLOGICAL CONDITIONS AND AEROSOL POLLUTION OVER THE CITY OF KEMEROVO

Yu.S. Balin, T.V. Vil'de, V.E. Zuev, N.P. Krasnenko, V.N. Molchanov, I.A. Razenkov, and M.G. Fursov

*Institute of Atmospheric Optics,
Siberian Branch of the Academy of Sciences of the USSR, Tomsk
Received February 15, 1990*

Results from experimental studies of the temperature stratification of the atmospheric boundary layer and the aerosol field distributions by an acoustic locator and an aerosol lidar are presented. The summertime atmospheric stability is estimated. Statistical parameters of the atmospheric temperature inversion levels are presented. Application of combined lidar and acoustic techniques to remote sensing of the atmosphere is shown to be quite effective for monitoring atmospheric pollution in urban areas.

The scale of atmospheric pollution of major industrial centers continues to increase, oftentimes reaching critical levels. The presence of toxic microelements in aerosol particles as part of the overall anthropogenic pollution makes these pollutants particularly detrimental to public health.

The existing systems for controlling urban atmospheric pollution are based on observations from networks of surface sensors deployed at separate urban sites, their data subject to subsequent laboratory analysis. Meanwhile, comprehensive operational information on the vertical stratification of meteorological parameters and on the spatial-temporal distribution of pollutants in urban atmosphere up to at least 0.5–1.0 km in altitude is needed for dedicated nature conservation activities. Information of that kind must include such characteristics of smoke plumes as their spatial (vertical and horizontal) extension, and aerosol mass concentrations in local air parcels at the mouth of the source and at large distances from it.

Even when industrial enterprises stick to norms of maximum permissible emissions, excessive concentrations of harmful pollutants in the lower atmosphere may result from adverse meteorological conditions, when strong vertical movements and mixing of the air are absent. Therefore, to assess the degree of atmospheric stability, i.e., the capacity of the atmosphere to disperse polluting emissions, one needs operational data on the vertical temperature-wind stratification of the atmosphere.

The formulation of such a task was decisive in the choice of instrumentation for an expedition of the Institute of Atmospheric Optics, which, was organized to study the state of the urban atmosphere over Kemerovo. Dangerous ecological situations have been regularly occurring of late in that city, which are produced by stable temperature inversions which set in during the spring and summer seasons and have the effect of accumulating pollutants in the lower at-

mospheric layers. The expedition took place during June 15–29, 1988.

The instrumentation of the expedition included lidars for monitoring gas and aerosol composition of the atmosphere, an acoustic locator, and an aircraft laboratory. The airborne studies gave an overall picture of the spatial aerosol distribution above the city, and made it possible to select an area of maximum atmospheric pollution for deploying the surface instrumentation. This paper presents some results of the aerosol field observations obtained with the help of the LOZA-3 lidar² and results of monitoring the temperature stratifications using the MAL-2 acoustic locator.³

The acoustic locator operated in the monostatic regime, sensing the atmosphere at 1, 1.5, and 2 KHz. The emitted pulses reached a 0.5–1.0 km ceiling at a spatial resolution of 34 m, and the sensing period was 6 seconds. The temperature stratification was continuously recorded in real time to a facsimile instrument. An example of such a facsimile recording is presented in Fig. 1 with the altitude plotted along the ordinate and the time — along the abscissa. The amplitude of the recorded acoustic signal is presented as a proportional darkening in the record and depends on the intensity of the temperature inhomogeneities.

From the very moment the measurements started (at 4 a.m.) two types of inversion were observed: a surface inversion — up to 150 m (the horizontal darkened layer) and an elevated inversion — alternately rising and falling (tilted darkened layers). After sunrise, from approximately 08:20 LT, convective fluxes began to develop due to surface heating; they gradually reached a height of 180–200 m and formed a mixing layer. Such records make it possible to monitor atmospheric stratification and to identify unfavorable meteorological situations which precipitate build-up of excessive pollutant concentrations. A discussion of the problem of the interpretation of such records may be found in Ref. 3.

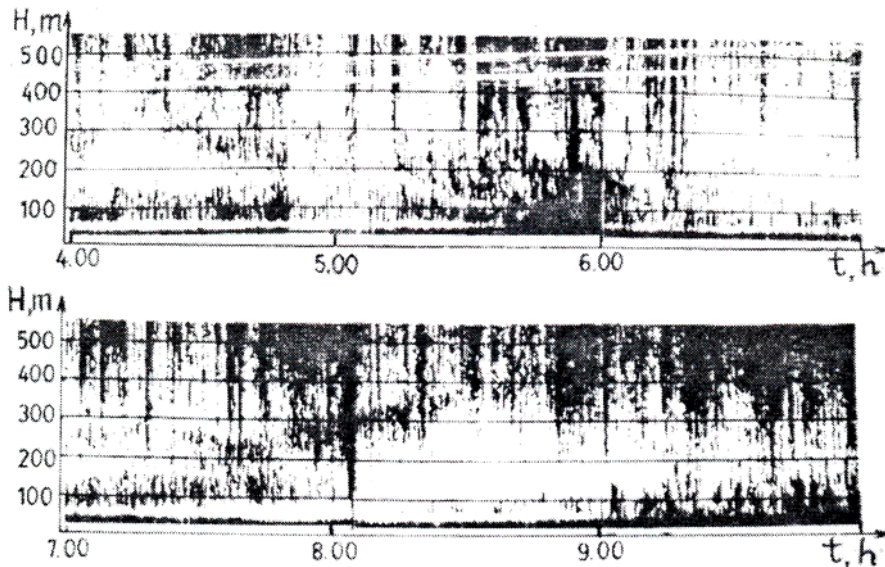


FIG. 1. Spatial-temporal record of the atmospheric temperature stratification, 0–500 m, June 6, 1988

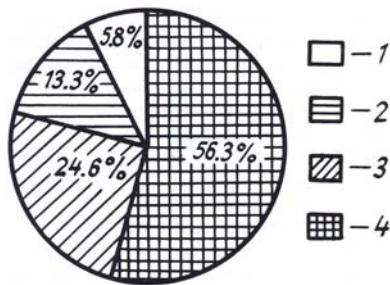


FIG. 2. Atmospheric temperature stratification classes: 1) neutral; 2) convective regime; 3) surface inversion; 4) elevated inversion or mixed.

The accumulated experimental data were then analyzed to obtain a general picture of atmospheric stability (the total operating time of the locator was 94 hours). During that observation period various atmospheric situations were identified: unstable atmosphere (developed convective turbulence), neutral situation (the atmospheric temperature gradient approximately equal to dry adiabatic vertical gradient), stable (surface and elevated temperature inversions or both types of inversion simultaneously present). Percentages of these atmospheric states for the entire observational series are shown in Fig. 2.

As can be seen from the presented data, temperature inversions had formed in approximately 81% of the cases, resulting in stable stratifications, causing pollutants to accumulate in the urban atmosphere. The number of elevated inversions during which meteorological conditions became most unfavorable, exceed 50% of the total. The principal characteristics of the atmospheric inversion, as is well known, are its top and bottom altitudes. The inversion forming at various elevations with respect to pollution-emitting smoke stacks of fixed height variously affect the build-up of urban emissions in the atmosphere.

Figure 3 presents normalized histograms of the top and bottom altitudes of the elevated inversion and also of the top of the surface inversion. It can be seen from these histograms that (see Fig. 3a) the top of the elevated inversion was at all times above 100 m, and, although it remained mostly in the 100–200 m range, it sometimes reached as high as 500 m. The distribution of the bottom heights of the elevated inversion was significantly narrower, 50–100 m above the ground. The top height of the surface inversion did not, as a rule, exceed 200 m.

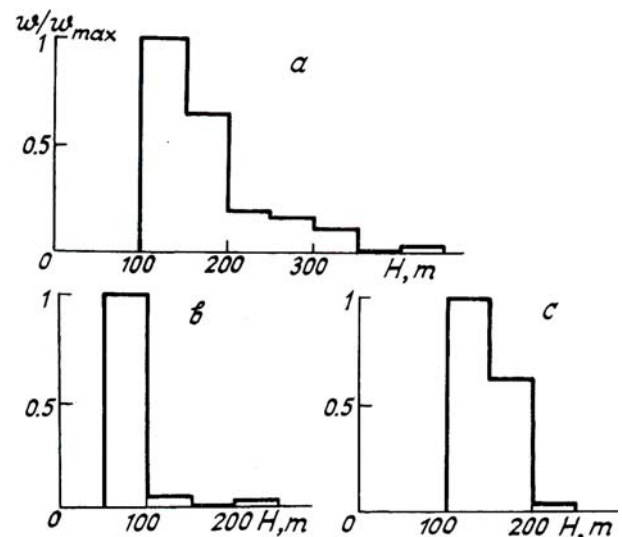


FIG. 3. Histograms of the top and bottom heights of the temperature inversions: a) elevated inversion, top; b) elevated inversion, bottom; c) surface inversion, top.

Results of statistical processing of the boundary heights of both types of inversions are given in Table I.

Note that heights below 50 m were left out of processing since they were in the acoustic locator "dead zone". Therefore elevated temperature inversions with bottoms below 50 m were conditionally classified as surface ones.

The results presented in Table I show that the average elevated inversion depth during the observation period was 81.3 m. As compared to the surface inversions the elevated ones displayed higher variability in the vertical.

Thus a general overview of the atmospheric stability situations over Kemerovo clearly indicates frequent temperature inversions with low, fairly stable vertical boundaries.

In combination with low smoke stacks (50–120 m) this explains, to a large extent, the ecologically unfavorable situation in the industrial areas of the town: smoke plumes are trapped inside temperature inversions, thus contributing to excessive pollution of the atmospheric surface layers. This result is supported by data from lidar soundings of the industrial aerosol fields.

TABLE I.

Statistical characteristics of temperature inversion boundaries, (Kemerovo, June 1988).

Parameter	Average altitude, m	Rms deviation, m	Variation coefficient, %
Upper boundary of elevated inversion	161.9	62.1	38
Lower boundary of elevated inversion	80.6	38.6	48
Upper boundary of surface inversion	136.6	26.7	20

The LOZA-3 scanning laser locator ($\lambda = 0.53 \mu\text{m}$) was positioned 1.2–1.5 km from a group of pollution sources and performed atmospheric sensing at 6 Hz frequency. The azimuth observation sector was usually 100–130°. The vertical sighting sector did not exceed 30–50° which allowed the laser beam to reach the tops of the smoke plumes. In the day time the operator using a TV camera could directly observe the investigated aerosol field, visually determining the sighting sectors.

The system for lidar control and data recording and processing is built around an "Elektronika-60" microcomputer which is configured for peripheral devices. Depending on the particular experimental tasks the control program accommodates several operational modes. When running the described experiment the operator introduced sector boundaries and the needed angular resolution into computer memory (the latter resolution might reach 0.1°). The moment the required angles are read into memory the

computer triggers the lidar and the atmospheric cross sections so obtained are recorded into computer memory over a uniform angular grid. The time required for scanning a horizontal atmospheric cross section within a 100° sector at a 1° angular step and a spatial resolution of 10–20 m is about 15 seconds. These data are then computer-processed and hardcopy spatial maps of the aerosol scattering coefficient distribution (aerosol mass concentration) are printed out by a dot-matrix printer.

In all about 60 horizontal and vertical cross sections of the aerosol field were obtained from the experiment phase. Figures 4a and 4b give typical examples of the aerosol field spatial distributions, obtained at a sighting angle of 6°, scanning in the horizontal at a 1° step at a spatial resolution of 20 m.

Figure 4a presents only that part of the sighting sector (with 60° coverage) in which the principal pollution sources are concentrated. Basically this example was chosen for the sake of graphic illustration: on that particular day (June 27, 1988) the meteorological situation was such that the pollution cloud was wind driven toward the lidar. In the same figure the spatial locations of the pollution sources identified by the lidar are schematically presented. In such a situation, and also with the wind direction reversed, one could reliably identify each separate pollution source by its own plume. If the wind direction was close to a line connecting several overlapping sources, such identification became much more difficult. This is illustrated by Fig. 4b (June 26, 1988) where the aerosol field cross section was obtained for the same angular sector. The cross sections in these figures were obtained during the morning hours, which were characterized by low winds and deep temperature inversions.

Figures 5a and 5b show vertical cross sections (i.e., sections 1 and 2 from Fig. 4b) for a surface temperature inversion reaching up to about 180 m. Facsimile atmospheric temperature records obtained by the acoustic locator are presented in the left parts of the same figures. In the presence of strong negative temperature gradients the atmosphere becomes very stable, eddy exchange is quite low, and the smoke plume should then remain at an approximately constant height, determined by the inversion level. This conclusion is supported by the results presented in Fig. 5. Simultaneously, a somewhat different picture is observed at a distance of 1000–1200 m from the lidar, near the sources themselves. Heat exhausted by individual enterprises in the area locally distorts the temperature inversion and forces emissions to lift up to about 300 m. At the same time higher aerosol concentrations are observed in the lower atmospheric layers there. In all the figures the aerosol layer distributions are presented as gradations in the backscattering coefficient (the mass concentration) shown as shades of black. The respective shade scales are shown in the upper part of figures.

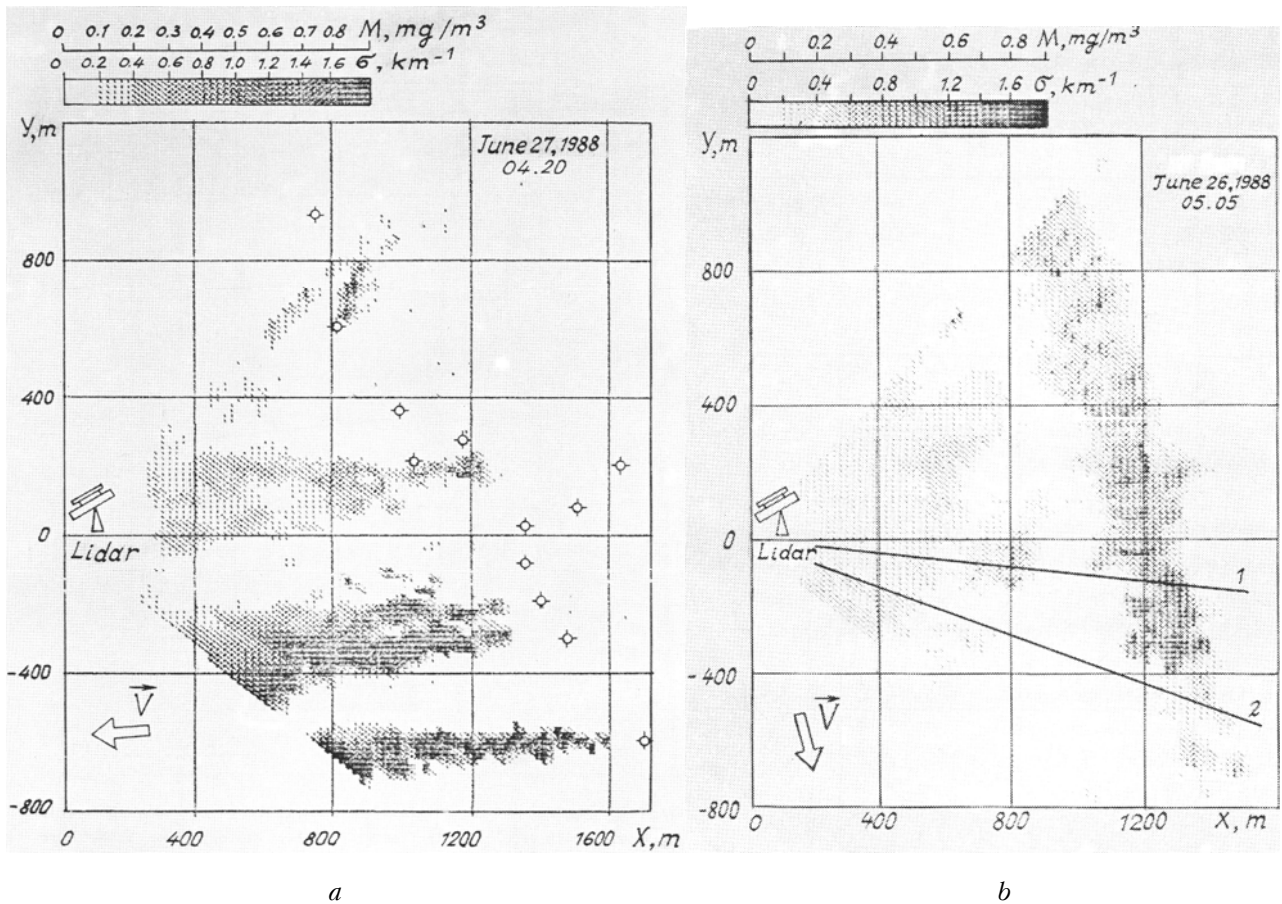


FIG. 4. Horizontal cross section of the aerosol field from the data obtained by the LOZA-lidar. Angular resolution — 1°; spatial resolution — 20 m; V — wind direction; ° — smokestacks; M — aerosol mass concentration; σ — scattering coefficient

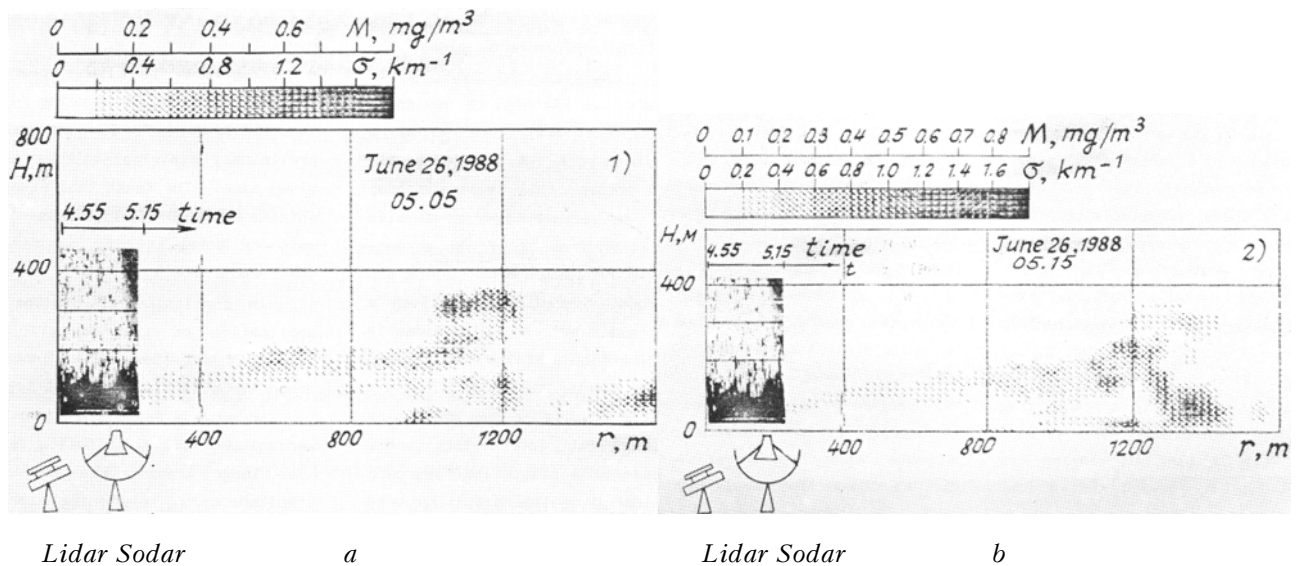


FIG. 5. Vertical cross section of the aerosol field from the data obtained by the LOZA-3 lidar in the presence of a surface temperature inversion (left record), by the acoustic locator (sodar): a — cross section 1 (Fig. 4b); b — cross section 2

Two principal methodological problems are encountered during lidar sensing of aerosol fields, especially those of industrial origin. The first consists in adequate choice or design of new algorithms for processing the lidar signals and retrieving the optical parameters of the aerosol field.

The widest practical application, at least for retrieving optical parameters along the sensing beam path, belongs to the Klett technique.⁴ This technique is based on assigning a priori the scattering coefficients within a finite sector of the beam path. As applied to the presently considered problem this technique has, however, failed. An apparently unrealistic distribution was obtained from it of the aerosol field in the form of alternating radial "black and white" bands of aerosol concentration. Such a result was explained by a significantly inhomogeneous distribution of the scattering coefficient within the viewing sector.

To obtain reliable results in the processing of lidar signals, optimal interference-stable algorithms which implement a statistical approach to the problem of lidar data interpretation were employed.⁵

A detailed treatment of this problem is outside the scope of the present article and requires special consideration.

The second, no less important, problem consists in estimating the aerosol mass concentration from data on its optical parameters. It was demonstrated in Ref. 6, which studied both theoretically and experimentally the coefficient p , which interrelates these characteristics, that under actual conditions one can expect significant variations in the value of $\mu = (0.52 \pm 0.34) \text{ mg} \cdot \text{km}/\text{m}^3$. The decisive role in this ambiguity is apparently played by the specific properties of urban aerosol, in particular, by its microoptical and microphysical parameters. However, Ref. 7 notes, overviewing and analyzing the results of investigations of various industrial smokes, that a high correlation (in excess of 0.9) is typical between the optical density and mass load of aerosol for each individual emission source. Moreover, for certain types of smokes the coefficient μ remains practically constant under various meteorological conditions. This is typical of those smokes whose average aerosol particle

radii correspond to values of the Mie parameter in the range $1 < \rho < 3-6$, and also for smokes containing weakly hygroscopic particles.

Therefore, to find a practical solution to the problem of estimating the aerosol mass concentration from optical measurements, preliminary empirical studies are needed in each given case. The least that needs to be done is to obtain an aerosol type classification for the emission sources being monitored (i.e., cement, dust, fuel, etc.).

In conclusion it can be stated that the application of lidar-acoustic techniques is a quite effective means for remote monitoring of urban air pollution.

In such a setup the lidar directly monitors aerosol particle distribution in urban atmospheres over large areas, while the acoustic locator, simultaneously monitoring the state of the atmosphere, makes it possible to track, on a real-time basis, its stability and localize temperature inversions, thus facilitating the forecast of unfavorable meteorological conditions that might result in excessive air pollution.

REFERENCES

1. V.E. Zuev, V.D. Belan, G.O. Zadde, et al., *Atm. Opt.*, **2**, No. 6, 523 (1989).
2. Yu.S. Balin, G.S. Bairashin, V.V. Burkov, et al., in: *Problem-Oriented Measurement-Calculational Complexes* (Nauka, Novosibirsk, 1986), pp. 65-71.
3. N.P. Krasnenko, *Acoustic Sensing of the Atmosphere* (Nauka, Novosibirsk, 1986), 167 pp.
4. J.D. Klett, *Appl. Opt.*, **22**, No. 4, 514-517 (1983).
5. G.M. Krekov, S.I. Kavkyanov, and M.M. Krekova, *Interpretation of Atmospheric Optical Sounding Signals* (Nauka, Novosibirsk, 1897), 184 pp.
6. V.E. Zuev, B.V. Kaul', I.V. Samokhvalov, et al., *Lidar Sensing of Industrial Aerosols* (Nauka, Novosibirsk, 1986), 188 pp.
7. D.B. Uvarov and G.P. Zhukov, *Trudy Inst. Eksp. Meteorol. Akad. Nauk SSSR* (Proc. of the Institute of Experimental Meteorology of the Acad. of Sci. of the USSR), Obninsk, No. 15 (60), 100-117 (1976).